The BFKL and GLDAP regimes for the perturbative QCD pomeron

N. N. Nikolaev and B. G. Zakharov

Institut für Kernphysik (Theorie), KFA Jülich D-52425, Jülich, Germany, and L. D. Landau Institute for Theoretical Physics, 117334 Moscow, Russia

V. R. Zoller

Institut für Kernphysik (Theorie), KFA Jülich D-52425, Jülich, Germany, and Institute for Theoretical and Experimental Physics, 117259 Moscow, Russia

(Submitted 11 January 1994)
Zh. Eksp. Teor. Fiz. **105**, 1498–1524 (June 1994)

The S-matrix of diffractive scattering is diagonalized in terms of the color dipole-dipole cross section. Recently, we have shown that the dipole cross section satisfies the generalized Balitskii–Fadin–Kuraev–Lipatov (BFKL) equation. In this paper we discuss the spectrum and solutions of our generalized BFKL equation with allowance for the finite gluon correlation radius R_c. The latter is introduced in a gauge-invariant manner. We present estimates of the intercept of the pomeron and find the asymptotic form of the dipole cross section. We consider the difference between the BFKL and Gribov–Lipatov–Dokshitzer–Altarelli–Parisi (GLDAP) evolutions and conclude that the GLDAP evolution remains a viable description of deep inelastic scattering well beyond the kinematical range of the HERA experiments. We suggest methods of measuring the pomeron intercept in the HERA experiments.

1. INTRODUCTION

The asymptotic behavior of high-energy scattering in perturbative QCD is usually discussed in terms of the Balitskii–Fadin–Kuraev–Lipatov (BFKL) pomeron.[1–3] The BFKL equation is the integral equation for the differential density of gluons, so that predicting observable quantities like total cross section is not sraightforward. Furthermore, the original BFKL equation is the scaling equation, and when discussing realistic QCD one encounters the difficult task of introducing an infrared cutoff in the BFKL equation. The scaling BFKL equation has a continuous spectrum and corresponds to the vacuum singularity described by a cut in the complex angular momentum plane. One of the pressing issues in the theory of the perturbative QCD pomeron is whether the infrared cutoff and the running QCD coupling can change the spectrum of the pomeron and produce isolated poles.

In this paper we discuss the spectrum and solutions of the generalized BFKL equation directly for the total cross section, derived by us recently.[4,5] Our equation allows us to introduce a finite correlation radius for the perturbative gluons in a gauge-invariant manner. The starting point of its derivation is the technique of multiparton lightcone wave functions, developed by two of the present authors.[4,6] The principal observation is that the transverse separations $\rho_{ij}=\rho_i-\rho_j$ and the lightcone momentum partitions z_i of partons in the many-body Fock state are conserved in the scattering process. Interaction of the $(n+2)$-parton Fock state is described by the lightcone wave function $\Psi_{n+2}(\rho_{n+2},z_{n+2},\ldots,\rho_1,z_1)$ and the $(n+2)$-parton cross section $\sigma_{n+2}(\rho_{n+2},\ldots,\rho_1)$, which are perturbatively calculable[4] (here n refers to the number of gluons in the Fock state).

To lowest order in perturbative QCD one starts with the $q\bar{q}$ Fock states of mesons (qqq state for the baryons) and with the scattering of the (A) projectile and (B) target color dipoles of transverse size $\mathbf{r}_A$ and $\mathbf{r}_B$ (here $\mathbf{r}_A,\mathbf{r}_B$ are the two-dimensional vectors in the impact parameter plane)

$$\sigma_0(\mathbf{r}_A,\mathbf{r}_B)=\frac{32}{9}\int\frac{d^2k}{(\mathbf{k}^2+\mu_G^2)^2}\alpha_S^2[1-\cos(\mathbf{k}\mathbf{r}_A)]\times[1-\cos(\mathbf{k}\mathbf{r}_B)]. \tag{1}$$

Here

$$\alpha_S(k^2)=\frac{4\pi}{\beta_0\log(k^2/\Lambda_{\rm QCD}^2)} \tag{2}$$

is the running strong coupling, $\beta_0=11-2/3N_f=9$ for $N_f=3$ active flavors, and in the integrand of the dipole-dipole cross section α_S^2 must be understood as

$$\alpha_S\left(\max\left\{k^2,\frac{C^2}{r_A^2}\right\}\right)\alpha_S\left(\max\left\{k^2,\frac{C^2}{r_B^2}\right\}\right),$$

where $C\approx 1.5$ (Ref. 6). The introduction of the infrared freezing of the running coupling and the correlation radius for gluons $R_c=1/\mu_G$ is discussed below. In terms of the dipole-dipole cross section (1) the perturbative part of the total cross section for the interaction of mesons A and B equals

$$\sigma^{(pt)}(AB)=\langle\langle\sigma(\mathbf{r}_A,\mathbf{r}_B)\rangle_A\rangle_B=\int dz_A d^2r_A dz_B d^2r_B|\Psi(z_A,\mathbf{r}_A)|^2|\Psi(z_B,\mathbf{r}_B)|^2\times\sigma_0(\mathbf{r}_A,\mathbf{r}_B). \tag{3}$$

 1063-7761/94/060806-15$10.00

The irrefutable advantage of the representation (3) is that it makes full use of the exact diagonalization of the scattering matrix in the dipole-size representation. [Hereafter we discuss $\sigma_0(\mathbf{r},\mathbf{R})$ averaged over the relative orientation of dipoles, as it appears in Eq. (3).] Notice the beam–target symmetry of the dipole-dipole cross section,

$$\sigma_0(\mathbf{r}_A,\mathbf{r}_B)=\sigma_0(\mathbf{r}_B,\mathbf{r}_A), \tag{4}$$

and of the representation (3).

The increase of the perturbative component of the total cross section comes from the increasing muliplicity of perturbative gluons in hadrons, $n_g \propto \log s$, times $\Delta\sigma_g$—the change in the dipole cross section in the presence of gluons: $\Delta\sigma^{(pt)} \sim n_g \Delta\sigma_g$. (Here s is the square of the c.m.s. energy.) The n-gluon Fock components of the meson give contributions $\propto \log^n s$ to the total cross section. The crucial observation is that the effects of higher-order Fock states of the interacting hadrons can be reabsorbed into the energy dependent dipole-dipole cross section with retention of the representation (3). This energy-dependent dipole cross section satisfies the generalized BFKL equation derived in Refs. 4 and 5, investigation of properties of which is the subject of the present paper. The presentation is organized as follows.

In Sec. 2 we briefly review the derivation of our generalized BFKL equation for the dipole cross and in Sec. 3 discuss its BFKL scaling limit. In Sec. 3 we also comment on the introduction of the infrared cutoff into the scaling BFKL equation. The subject of Sec. 4 is the conventional QCD evolution as the limiting case of our generalized BFKL equation. The impact of the finite correlation length for gluons and of the running QCD coupling on the spectrum of the generalized BFKL equation is discussed in detail in Sec. 5. Our principal conclusion is that the generalized BFKL kernel has a continuous spectrum, so that the partial waves of the scattering amplitude have a cut in the complex angular momentum plane. We also comment on the conditions under which the pomeron can have a discrete spectrum. In Sec. 6 we find the form of the dipole cross section for the rightmost singularity in the j-plane and its intercept as a function of the gluon correlation radius R_c. The subject of Sec. 7 is the transition from the Gribov–Lipatov–Dokshitzer–Altarelli–Parisi (GLDAP) evolution to the BFKL evolution with increasing energy. The beam–target symmetry of the dipole–dipole cross section and the admissible form of the boundary conditions for the generalized BFKL equation are discussed in Sec. 8. In Sec. 9 we comment on the restoration of the factorization property of the asymptotic cross section. In Sec. 10 we suggest practical methods of measuring the intercept of the pomeron in the HERA experiments on deep inelastic scattering. In the Conclusions we summarize our basic results.

2. GENERALIZED BFKL EQUATION FOR TOTAL CROSS SECTION

Now we sketch the derivation of our generalized BFKL equation[4,5] for total cross sections. Unless otherwise specified, we consider the contribution to the hadronic scattering from the exchange by the perturbative gluons and suppress the superscript (pt). The perturbative $q\bar{q}g$ Fock state generated radiatively from the parent color-singlet $q\bar{q}$ state of size $\mathbf{r}$ has the interaction cross section[4]

$$\sigma_3(r,\rho_1,\rho_2)=\frac{9}{8}\left[\sigma_0(\rho_1)+\sigma_0(\rho_2)\right]-\frac{1}{8}\sigma_0(r), \tag{5}$$

where $\rho_{1,2}$ are separations of the gluon from the quark and antiquark respectively, $\rho_2=\rho_1-\mathbf{r}$. (Hereafter we suppress the target variable r_B and for the sake of brevity use $r=r_A$.) The cross section $\sigma_3(r,\rho_1,\rho_2)$ has the gauge-invariance properties $\sigma_3(r,0,r)=\sigma_3(r,r,0)=\sigma_0(r)$ and $\sigma_3(0,\rho,\rho)=9/4\sigma_0(\rho)$ (Ref. 4). The former shows that when the gluon is sitting on top of the (anti)quark, the $qg(\bar{q}g)$ system is indistinguishable from the (anti)quark. The latter shows that the color-octet $q\bar{q}$ system of vanishing size is indistinguishable from the gluon, and 9/4 is the familiar ratio of the octet and triplet couplings. The increase of the cross section for the presence of gluons equals

$$\begin{aligned}\Delta\sigma_g(r,\rho_1,\rho_2)&=\sigma_3(r,\rho_1,\rho_2)-\sigma_0(r)\\&=\frac{9}{8}\left[\sigma_0(\rho_1)+\sigma_0(\rho_2)-\sigma_0(r)\right].\end{aligned} \tag{6}$$

The lightcone density of soft, $z_g \ll 1$, gluons in the $q\bar{q}g$ state derived in Ref. 4 equals

$$|\Phi_1(\mathbf{r},\rho_1,\rho_2,z_g)|^2=\frac{1}{z_g}\frac{1}{3\pi^3}\mu_G^2\left|g_S(r_1^{(\min)})K_1(\mu_G\rho_1)\frac{\rho_1}{\rho_1}-g_S(r_2^{(\min)})K_1(\mu_G\rho_2)\frac{\rho_2}{\rho_2}\right|^2. \tag{7}$$

Here $g_S(r)$ is the running color charge, $\alpha_S(r)=g_S^2(r)/4\pi$ is the running strong coupling, $r_{1,2}^{(\min)}=\min\{r,\rho_{1,2}\}$, $K_1(x)$ is the modified Bessel function, z_g is a fraction of the (lightcone) momentum of the $q\bar{q}$ pair carried by the gluon, and $\int dz_g/z_g=\log(s/s_0)=\xi$ is the parameter of the leading $\log(1/x)$ approximation and gives the usual logarithmic multiplicity of radiative gluons. The wave function (7) counts only the physical, transverse, gluons.[4]

If $n_g(r)$ is the number of perturbative gluons in the dipole $\mathbf{r}$,

$$n_g(r)=\int dz_g d^2\rho_1 |\Phi_1(\mathbf{r},\rho_1,\rho_2,z_g)|^2, \tag{8}$$

then the weight of the radiationless $q\bar{q}$ component will be renormalized by the factor $1-n_g(z,\mathbf{r})$. As a result, the total cross section with allowance for the perturbative gluons in the beam dipole A takes the form

$$\begin{aligned}\sigma(\xi,r)&=[1-n_g(z,\mathbf{r})]\sigma_0(r)\\&\quad+\int dz_g d^2\rho_1 |\Phi_1(\mathbf{r},\rho_1,\rho_2,z_g)|^2\sigma_3(r,\rho_1,\rho_2)\\&=\sigma_0(r)+\int dz_g d^2\rho_1 |\Phi_1(\mathbf{r},\rho_1,\rho_2,z_g)|^2\Delta\sigma_g(r,\rho_1,\rho_2)\\&=\sigma_0(r)+\sigma_1(r)\xi=[1+\xi\mathscr{K}\otimes]\sigma_0(r),\end{aligned} \tag{9}$$

where the kernel $\mathscr{K}$ is defined by[4,5]

$$\sigma_1(r)=\mathscr{K}\otimes\sigma_0(r)$$

$$=\frac{3}{8\pi^3}\int d^2\rho_1\mu_G^2\left|g_S(r_1^{(\min)})K_1(\mu_G\rho_1)\frac{\rho_1}{\rho_1}-g_S(r_2^{(\min)})\right.$$

$$\left.\times K_1(\mu_G\rho_2)\frac{\rho_2}{\rho_2}\right|^2[\sigma_0(\rho_1)+\sigma_0(\rho_2)-\sigma_0(r)]. \quad (10)$$

Equation (9) shows that the effect of gluons can be reabsorbed into the generalized, energy-dependent, dipole cross section $\sigma(\xi,r)$. To higher orders in ξ, this generalized dipole cross section can be expanded as

$$\sigma(\xi,r)=\sum_{n=0}\frac{1}{n!}\sigma_n(r)\xi^n,$$

where $\sigma_{n+1}=\mathscr{K}\otimes\sigma_n$, so that

$$\frac{\partial\sigma(\xi,r)}{\partial\xi}=\mathscr{K}\otimes\sigma(\xi,r) \quad (11)$$

is our generalization of the BFKL equation for the dipole cross section.

The color gauge invariance of the presented formalism is noteworthy. Firstly, the dipole-dipole cross section $\sigma_0(r_A,r_B)$ vanishes at $r_A\to 0$ or $r_B\to 0$, because gluons decouple from the color-singlet state of vanishing size. Secondly, for the same reason the wave function (7) vanishes at $r\to 0$. Thirdly, $\Delta\sigma_g(r,\rho_1,\rho_2)\to 0$ when $\rho_1\to 0$ (or $\rho_2\to 0$), since by color charge conservation the quark-gluon system with the gluon sitting on top of the (anti)quark is indistinguishable from the (anti)quark, and the interaction properties of such a $q\bar{q}g$ state are identical to that of the $q\bar{q}$ state. Therefore, our introduction of a finite correlation radius for gluons $R_c=1/\mu_G$, which takes care of the perturbative gluons not propagating beyond the correlation radius R_c, is perfectly consistent with the gauge invariance. For instance, Eq. (10) supports the gauge invariance constraint $\sigma_n(r)\to 0$ at $r\to 0$, to all orders n. (We do not have a complete proof of the gauge invariance, though. Neither can we prove that our prescription is unique.)

The renormalization of the weight of the radiationless $q\bar{q}$ Fock state in Eq. (9) in a simple and intuitively appealing form takes care of the virtual radiative corrections (in the BFKL formalism[1,2] these very radiative corrections are responsible for the reggeization of gluons). Notice, that although the multiplicity of radiative gluons $n_g(r)$, which appeared in the intermediate stage of the derivation of our Eq. (10), is formally divergent, the generalized dipole cross section $\sigma(\xi,r)$ and Eqs. (10) and (11) are both ultraviolet- and infrared-finite.

3. THE BFKL SCALING LIMIT

In the BFKL scaling limit of $r,\rho_1,\rho_2\ll R_c$ and for fixed α_S,

$$\mu_G^2\left|K_1(\mu_G\rho_1)\frac{\rho_1}{\rho_1}-K_1(\mu_G\rho_2)\frac{\rho_2}{\rho_2}\right|^2=\frac{r^2}{\rho_1^2\rho_2^2}, \quad (12)$$

the kernel $\mathscr{K}$ becomes independent of the gluon correlation radius R_c and with fixed α_S it takes on the scale-invariant form. The corresponding eigenfunctions of Eq. (11) are

$$E(\omega,\xi,r)=(r^2)^{1/2+\omega}\exp[\xi\Delta(\omega)] \quad (13)$$

with the eigenvalue (intercept) [here $\mathbf{r}=r\mathbf{n}$, $\rho_1=r\mathbf{x}$ and $\rho_2=r(\mathbf{x}+\mathbf{n})$]

$$\Delta(\omega)=\lim_{\varepsilon\to 0}\frac{3\alpha_S}{2\pi^2}\int d^2x\frac{2(\mathbf{x}^2)^{1/2+\omega}-1}{[\mathbf{x}^2+\varepsilon^2][(\mathbf{x}+\mathbf{n})^2+\varepsilon^2]}$$

$$=\frac{3\alpha_S}{\pi}\int_0^1 dz\frac{z^{1/2-\omega}+z^{1/2+\omega}-2z}{z(1-z)}$$

$$=\frac{3\alpha_S}{\pi}\left[2\Psi(1)-\Psi\left(\frac{1}{2}-\omega\right)-\Psi\left(\frac{1}{2}+\omega\right)\right]. \quad (14)$$

Here $\Psi(x)$ is the digamma function, and we have indicated the regularization which preserves the symmetry of the kernel $\mathscr{K}$. The final result for $\Delta(\omega)$ coincides with eigenvalues of the BFKL equation found in Refs. 1–3. The solution (13) corresponds to the singularity in the complex-j plane, located at $j=1+\Delta(\omega)$. The rightmost singularity is located at $j=\alpha_{\mathbf{IP}}=1+\Delta_{\mathbf{IP}}$, where

$$\Delta_{\mathbf{IP}}=\Delta(0)=\frac{12\log 2}{\pi}\alpha_S. \quad (15)$$

When ω is real and varies from $-1/2$ to 0 and to $1/2$, the intercept $\Delta(\omega)$ is also real and varies from $+\infty$ down to $\Delta(0)=\Delta_{\mathbf{IP}}$ and back to $+\infty$, along the cut from $j=1+\Delta_{\mathbf{IP}}$ to $+\infty$ in the complex angular momentum j plane. If $\omega=i\nu$ holds and ν varies from $-\infty$ to 0 and to $+\infty$, then the intercept $\Delta(i\nu)$ is again real and varies from $-\infty$ up to $\Delta(0)=\Delta_{\mathbf{IP}}$ and back to $-\infty$, along the cut from $j=-\infty$ to $j=1+\Delta_{\mathbf{IP}}$ in the complex j-plane. The choice of the latter cut is appropriate for the Regge asymptotics at $\xi\gg 1$ and the counterpart of the usual Mellin representation is

$$\sigma(\xi,r)=\int_{-\infty}^{+\infty}d\nu f(\nu)E(i\nu,r,\xi)$$

$$=r\int_{-\infty}^{+\infty}d\nu f(\nu)\exp[2i\nu\log(r)]\exp(\Delta(i\nu)\xi). \quad (16)$$

The Mellin transform is obtained from Eq. (16) if one changes the integration variable from ν to the angular momentum $j=1+\Delta(i\nu)$. The spectral amplitude $f(\nu)$ is determined by the boundary condition $\sigma(\xi=0,r)$:

$$f(\nu)=\frac{1}{\pi}\int dr\frac{\sigma(0,r)}{r^2}\exp[-2i\nu\log(r)]. \quad (17)$$

Eqs. (16) and (17) give a nontrivial connection between the r-dependence of the total cross section and its energy dependence. In the BFKL scaling regime, the rightmost j-plane singularity corresponds to the asymptotic dipole cross section $\sigma_{\mathbf{IP}}(\xi,r)=\sigma_{\mathbf{IP}}(r)\exp(\xi\Delta_{\mathbf{IP}})$, where

$$\sigma_{\mathbf{IP}}(r)\propto r. \quad (18)$$

A more direct correspondance between equations (10) and (11) in the scaling limit of $\mu_G \to 0$ and the conventional BFKL equation can be established if one rewrites Eqs. (10) and (11) as an equation for the function

$$g(\xi,r)=\frac{3\sigma(\xi,r)}{\pi^2\alpha_S r^2}, \tag{19}$$

which in the BFKL scaling limit is simply the density of gluons $g(x,k^2)$ at the Bjorken variable $x=x_0\exp(-\xi)$ and with virtuality $k^2\sim 1/r^2$, where $x_0\sim 0.1-0.01$ corresponds to the onset of the leading $\log(1/x)$ approximation (the relation (19) holds also for the running strong coupling $\alpha_S=\alpha_S(r)$; for the detailed derivation see Refs. 4,7). The transformation from the size-**r** representation to the momentum-**p** representation can easily be performed making use of the conformal symmetry of the BFKL equation.[3] Namely, by virtue of the conformal symmetry **r** can easily be traded for **p** and $\sigma(\xi,r)$ can be traded for $g(\xi,p^2)$, with the result

$$\frac{\partial g(\xi,p^2)}{\partial\xi}=\frac{3\alpha_S}{2\pi^2}\int d^2k\,\frac{\mathbf{p}^2}{\mathbf{k}^2(\mathbf{p}-\mathbf{k})^2}\,[g(\xi,k^2) +g(\xi,(\mathbf{p}-\mathbf{k})^2)-g(\xi,p^2)]. \tag{20}$$

The factor p^2 in the integrand of (20) is crucial for supporting the gauge invariance constraint $g(\xi,p^2)\to 0$ in the limit $p^2\to 0$, which is the counterpart of the gauge invariance constraint $\sigma(\xi,r)\to 0$ in the limit $r\to 0$ in the **r**-representation. If one introduces $\psi(\xi,k^2)=g(\xi,k^2)/k^2$, then the original form of the BFKL equation will be recovered from Eq. (20) [in the scaling limit $\psi(\xi,k^2)$ satisfies the same equation as the more often considered $\partial g(\xi,k^2)/\partial k^2$].

Introduction of the infrared regularization into the BFKL scaling equation (20) is one of the pressing issues in the theory of the perturbative QCD pomeron. We are going to use neither Eq. (20) nor any of its modifications to be discussed below; we resort to Eqs. (10) and (11), which allow effects of both the gluon correlation radius R_c and the running strong coupling to be treated in a consistent and manifestly gauge-invariant manner. Nevertheless, in order to establish a connection with the existing literature, we comment on the infrared regularization of the BFKL Eq. (20) in the momentum representation.

Our form (20) of the BFKL equation is more convenient for these purposes, as it allows the clearcut separation of propagators $1/\mathbf{k}^2$ and $1/(\mathbf{p}-\mathbf{k})^2$ from the factor $\mathbf{p}^2$ in the nominator in Eq. (20). The latter, like the factor r^2 in Eq. (12), has its origin in cancellations of the radiation of soft gluons by the color singlet states. Therefore, the infrared regularization of Eq. (20) which plausibly respects the gauge invariance, is the substitution

$$\frac{\mathbf{p}^2}{\mathbf{k}^2(\mathbf{p}-\mathbf{k})^2}\Rightarrow\frac{\mathbf{p}^2}{[\mathbf{k}^2+m^2][(\mathbf{p}-\mathbf{k})^2+m^2]}, \tag{21}$$

which treats the both gluon propagators on the equal footing. In the scaling limit of $p^2\gg m^2$, the function $\psi(\xi,p^2)=g(\xi,p^2)/(p^2+m^2)$ is similar to, and satisfies the same equation as, $\partial g(\xi,p^2)/\partial p^2$. The equation for $\psi(\xi,p^2)$, which follows from (20) subject to the substitution (21), reads

$$\begin{aligned}\frac{\partial\psi(\xi,p^2)}{\partial\xi}&=\frac{3\alpha_S}{2\pi^2}\frac{\mathbf{p}^2}{\mathbf{p}^2+m^2}\int d^2k\left[\frac{\psi(\xi,k^2)}{(\mathbf{p}-\mathbf{k})^2+m^2}\right.\\ &\left.+\frac{\psi(\xi,(\mathbf{p}-\mathbf{k})^2)}{\mathbf{k}^2+m^2}-\frac{(p^2+m^2)\psi(\xi,p^2)}{[(\mathbf{p}-\mathbf{k})^2+m^2][\mathbf{k}^2+m^2]}\right]\\ &=\frac{3\alpha_S}{\pi^2}\frac{\mathbf{p}^2}{\mathbf{p}^2+m^2}\int d^2k\left[\frac{\psi(\xi,k^2)}{(\mathbf{p}-\mathbf{k})^2+m^2}\right.\\ &\left.-\frac{(p^2+m^2)\psi(\xi,p^2)}{[(\mathbf{p}-\mathbf{k})^2+m^2][\mathbf{k}^2+(\mathbf{p}-\mathbf{k})^2+2m^2]}\right].\end{aligned} \tag{22}$$

The asymmetric form in the second line of Eq. (22) is obtained from the symmetric form in the first line of Eq. (22) if one uses the identity[2]

$$\begin{aligned}&\int\frac{d^2k}{[\mathbf{k}^2+m^2][(\mathbf{p}-\mathbf{k})^2+m^2]}\\ &\quad=2\int\frac{d^2k}{[\mathbf{k}^2+m^2][(\mathbf{p}-\mathbf{k})^2+\mathbf{k}^2+2m^2]}.\end{aligned} \tag{23}$$

(An erroneous form of this identity is cited in Ref. 8). The asymmetric form of Eq. (22) at $m^2=0$ is precisely the Balitskii-Lipatov form[2] of the BFKL equation, which is the one customarily used in the recent literature.

One often imposes on this asymmetric version of the BFKL equation the infrared cutoff $k^2\geqslant k_0^2$ (Refs. 9–11), which is illegitimate. Indeed, such a cutoff does not ensure, and as matter of fact manifestly breaks, the condition of the identical infrared cutoff of different gluon propagators, as it breaks the initial symmetry property of the BFKL Eq. (20) (for a similar criticism of the Collins–Kwiecinski[9] (CK) sharp cutoff $k^2\geqslant k_0^2$ see also Collins and Landshoff[10]). Furthermore, such a cutoff is evidently suspect from the point of view of gauge invariance. One must rather use Eq. (22) which introduces the infrared regularization with retention of the symmetric cutoff of the gluon propagators and in the manifestly gauge invariant manner. Balitskii and Lipatov[2] did not encounter these problems, as they introduce the massive vector mesons in a consistent manner, using the spontaneous breaking of gauge symmetry. Introduction of massive gluons into the BFKL equation was also discussed by Ross and Hancock.[11] The Ross–Hancock prescription is different from ours in Eq. (22), manifestly breaks the symmetry of the cutoff of gluon propagators, and, in contrast to Eq. (22), does not support the $\mathbf{p}^2\to 0$ gauge invariance constraints.

4. THE GLDAP LIMIT

The limit of large but finite ξ and very small $r^2\ll R^2$ is often referred to as the Double-Leading-Logarithmic Approximation (DLLA). Here R is either the target size, $R\sim r_B$ or the correlation radius R_c if $R_c<r_B$. This is the limit typical of deep inelastic scattering, and it is usually described by the GLDAP evolution equations.[12] Introduction of the gluon correlation radius R_c and of the running

QCD coupling poses no problems in the DLLA. In the DLLA we have $\xi=\log(x_0/x)$, where x is the Bjorken variable, and $x_0\lesssim 0.1-0.01$ is the threshold for the leading-log$(1/x)$ approximation. The BFKL equation contains the GLDAP equation as the limiting case. In the DLLA the kernel $\mathscr{K}$ takes a particularly simple form[4]

$$\sigma_{n+1}(r)=\mathscr{K}\otimes\sigma_n(r)=\frac{3r^2\alpha_S(r)}{\pi^2}\int_{r^2}^{R^2}\frac{d^2\rho}{\rho^4}\sigma_n(\rho), \tag{24}$$

which is equivalent to the GLDAP evolution equation. The dominant contribution comes from the DLLA ordering of sizes $r^2\ll\rho^2\ll R^2$, which justifies factoring out $\alpha_S(r)$ in Eq. (24). In the same DLLA the boundary condition, the dipole–dipole cross section (3), equals

$$\sigma(\xi=0,r)=\sigma_0(r,R)\approx Cr^2\alpha_S(r)L(R,r), \tag{25}$$

where $L(R,r)$ is the parameter of the leading-log(r^2) approximation (the leading-log(Q^2) approximation in the more conventional momentum representation),

$$L(R,r)\approx\log\left[\frac{\alpha_S(R)}{\alpha_S(r)}\right]. \tag{26}$$

Iterations of Eq. (24) subject to the boundary condition (25) give the DLLA solution[4]

$$\sigma_{n+1}(r)=\mathscr{K}\otimes\sigma_n(r)=\frac{1}{n+1}\frac{12}{\beta_0}L(R,r)\sigma_n(r). \tag{27}$$

The corresponding generalized dipole cross section has the DLLA asymptotic form

$$\sigma_{\mathrm{DLLA}}(\xi,r)=\sigma(0,r)\sum_{n=0}\frac{\eta^n}{n!(n+1)!}$$

$$\sim r^2\alpha_S(r)L(r,R)\frac{\exp(2\sqrt{\eta})}{\sqrt{\eta}}, \tag{28}$$

where η is the expansion parameter of DLLA, which is a product of the leading-log(s) and the leading-log(r^2) expansion parameters:

$$\eta=\frac{12}{\beta_0}\xi L(r,R)=\frac{4}{3}\xi L(r,R). \tag{29}$$

Notice that the DLLA solution implicitly invovles an assumption that at large $r\sim R$, the cross section $\sigma_{\mathrm{DLLA}}(\xi,r)$ is approximately constant.

The large-n behavior of the DLLA iterations (27) must be compared to

$$\sigma_{n+1}(r)=\Delta_{\mathrm{IP}}\sigma_n(r) \tag{30}$$

for the leading BFKL solution, which suggests the criterion for the breaking of the DLLA and/or GLDAP evolution: At large η the DLLA cross section (28) is dominated by the contribution from large $n\sim\sqrt{\eta}$. The DLLA-to-GLDAP evolution breaks when

$$\frac{L(R,r)}{n}\approx\frac{L(R,r)}{\sqrt{\eta}}\lesssim\frac{3}{4}\Delta_{\mathrm{IP}}. \tag{31}$$

The pattern of this DLLA breaking in the case of running $\alpha_S(r)$ will be discussed in more detail below. Here we only wish to emphasize that in the physically interesting case of the running coupling and of finite correlation radius for the perturbative gluons R_c the intercept Δ_{IP} is the constant, which does not depend on r. Therefore, the boundary line $x=x_c(r)$ in the (r,ξ) plane between the BFKL evolution and the GLDAP evolution to DLLA is given by

$$\log\left(\frac{x_0}{x_c(r)}\right)=\frac{4}{3\Delta_{\mathrm{IP}}^2}\log\left[\frac{1}{\alpha_S(r)}\right]. \tag{32}$$

It is different from the much discussed erroneous boundary suggested in Ref. 8. We shall comment more on the transition from the DLLA to GLDAP evolution to the BFKL evolution below; for now we concentrate on the investigation of the spectrum and eigenfunctions of our generalized BFKL equation.

5. THE SPECTRUM AND EIGENFUNCTIONS OF THE GENERALIZED BFKL EQUATION

5.1. The Green's function, diffusion, and the "Schrödinger" equation

The generic solution of Eq. (11) can be written as

$$\sigma(\xi,r)=r\int\frac{dr'}{r'^2}K(\xi,r,r')\sigma(\xi=0,r'), \tag{33}$$

where in the BFKL regime the evolution kernel (Green's function) equals

$$K(\xi,r,r')=\frac{1}{\pi}\int d\nu\exp\left[2i\nu\log\frac{r}{r'}\right]\exp[\xi\Delta(i\nu)]. \tag{34}$$

Since $\Delta(i\nu)$ has the maximum at $\nu=0$,

$$\Delta(i\nu)=\Delta_{\mathrm{IP}}-\frac{1}{2}\Delta''(0)\nu^2, \tag{35}$$

the large-ξ behavior of the Green's function can be evaluated in the saddle-point approximation:

$$K(\xi,r,r')\propto\frac{\exp(\Delta_{\mathrm{IP}}\xi)}{\sqrt{\xi}}\exp\left[-\frac{(\log r^2-\log r'^2)^2}{2\xi\Delta''(0)}\right]. \tag{36}$$

Since the BFKL eigenfunctions (13) are oscillating functions of r, *á priori* it is not obvious that an arbitrary solution (16) will be positive-valued at all ξ and r. The BFKL kernel $K(\xi,r,r')$ of Eq. (34) is manifestly positive-valued at large ξ, so that starting with the positive-valued $\sigma(0,r)$ one obtains the positive-valued asymptotic cross section $\sigma(\xi,r)$.

The "diffusion" kernel (34) makes it obvious that the BFKL scaling approximation is not self-consistent in the realm of realistic QCD: starting with $\sigma(\xi=0,r)$, which was concentrated at the perturbative small $r\lesssim R\ll R_c$, one ends up at large ξ with $\sigma(\xi,r)$, which extends up to the nonperturbative $r\sim R\exp[\sqrt{\xi\Delta''(0)}]>R_c$. Therefore, introduction of a certain infrared regularization in the form of a finite gluon correlation length R_c is inevitable; hereafter we concentrate on effects of finite R_c on the intercept Δ_{IP}. In-

terpretation of $\mu_G = 1/R_c$ as an effective mass of the gluon suggests the infrared freezing of the strong coupling $\alpha_S(r)$ at $r > R_f \sim R_c$. In the numerical analysis we use the running coupling

$$\alpha_S(r) = \frac{4\pi}{\beta_0 \log(C^2/\Lambda^2_{\rm QCD} r^2)}, \tag{37}$$

where[6] $C \approx 1.5$. At large r we impose the simplest freezing $\alpha_S(r > R_f) = \alpha_S^{(fr)} = 0.8$. This corresponds to the freezing radius $R_f \approx 0.42$ F and/or the freezing momentum $k_f \approx 0.72$ GeV/c in the momentum representation (2). The more sophisticated smooth freezing can easily be considered, but it will be obvious that our principal conclusions do not depend on the form of the freezing. The gluon correlation radius R_c and the freezing coupling provide the minimal infrared regularization of the perturbation theory, and in the sequel we assume that the so-regularized generalized BFKL Eqs. (10) and (11) is applicable at both small and large radii r.

Although only the case of $R_c \approx R_f$ is of the physical interest, the study of (albeit unphysical) limiting cases $R_f \to 0$ at finite R_c, and of finite R_f at $R_c \to \infty$, is instructive for the insight into how the spectrum of the j-plane singularities is modified by the infrared regularization. The corresponding analysis is greatly facilitated by the observation, that in view of Eqs. (33) and (36) the large-ξ behavior of solutions of the BFKL limit of Eq. (11) is similar to the large-ξ behavior of solutions of the "Schrödinger" equation

$$\left[-\frac{\Delta''(0)}{2}\frac{\partial^2}{\partial z^2} + V(z)\right]\Phi = -\frac{\partial}{\partial \xi}\Phi = \varepsilon\Phi \tag{38}$$

for a particle of mass $M = 1/\Delta''(0)$ in the potential $V(z) = -\Delta(0)$. Here we have written $z = \log r^2$, the "wavefunction" is $\Phi(z,\xi) = \sigma(\xi,r)/r$ and the intercept equals the "energy" ε taken with the minus sign.

5.2. Finite correlation radius R_c, fixed coupling α_S

The first limiting case $R_f \to 0$ corresponds to introduction of a finite gluon correlation radius R_c at fixed α_S. In this limiting case the intercept $\Delta_{\rm IP}$ will still be given by the BFKL formula (15). Indeed, on the infinite semiaxis $\log r < \log R_c$ the kernel $\mathscr{K}$ retains its scaling properties, the corresponding eigenfunctions will be essentially identical to the set (13), the spectrum of eigenvalues will be continuous and the cut in the j-plane will be the same as at $R_c \to \infty$. This is particularly obvious from the Schrödinger Eq. (38), since on the semiaxis $z < z_c = \log R_c^2$ the potential $V(z) = -\Delta_{\rm IP}$ is flat, and the corresponding Schrödinger operator (38) has a continuous spectrum starting with the minimum energy $\varepsilon = -\Delta_{\rm IP}$. Evidently, this property of the spectrum of the Schrödinger operator (38) does not depend on the details of how the gluon correlation length R_c is introduced. This is a reason why the similar conclusion on the spectrum of the infrared-cutoff BFKL equation was reached in Ref. 9 in a model with the sharp $k^2 \geqslant k_0^2$ cutoff in the momentum representation criticized above.

The behavior of solutions at large $r \gg R_c$ requires special investigation. In this region the term $\propto K_1(\mu_G\rho_1)K_1(\mu_G\rho_2)$ in the kernel $\mathscr{K}$ is exponentially small, which is related to the exponential decay of the correlation function (the propagator) of perturbative gluons. [Such an exponential decay of the gluon correlation function with the correlation radius $R_c = 0.2$–0.4 F is suggested by the lattice QCD studies; for a review see Ref. 13. We recall that $K_1(x)$ in the kernel $\mathscr{K}$ comes from the gradient of the gluon correlation function $\propto K_0(x)$]. Then, at large r the kernel $\mathscr{K}$ of our Eq. (11) will be dominated by the contributions from $\rho_1 \lesssim R_c \ll \rho_2 \approx r$ and from $\rho_2 \lesssim R_c \ll \rho_1 \approx r$, will have a limiting value which does not depend on r, and Eq. (11) takes the form

$$\sigma_{n+1}(r) = \frac{3\alpha_S}{\pi^3}\int d^2\rho_1 \mu_G^2 K_1^2(\mu_G\rho_1) \times [\sigma_n(\rho_1) + \sigma_n(\rho_2) - \sigma_n(r)]. \tag{39}$$

This equation has a continuum of solutions with the large-r behavior of the form

$$E_+(\beta,\xi,r) = [a(\beta) + \exp(i\beta\mu_G r)]\exp[\delta(\beta)\xi]. \tag{40}$$

[Apparently, one can put $a(\beta) = 0$, but this is unimportant for the subsequent analysis.]

When continued to small r through the region $r \sim R_c$, the plane waves in the linear-r space transform into plane waves in log r^2-space (times the overall factor r),

$$E(i\nu,\xi,r) = r\exp(i\nu \log r^2)$$

of Eq. (13), so that $\delta(\beta) = \Delta(i\nu)$. Evidently, the two real and node-free solutions with $\nu = 0$ and $\beta = 0$ must match each other, so that the rightmost j-plane singularity with the intercept $\Delta_{\rm IP}$ Eq. (15) must correspond to $\sigma_{\rm IP}(r) \propto r$ at $r \ll R_c$ and $\sigma_{\rm IP}(r) \propto$ const at $r \gg R_c$. We wish to emphasize that although such a $\sigma_{\rm IP}(r)$ extends to large r, Eq. (39) makes it obvious that the intercept $\Delta_{\rm IP}$ is controlled by the behavior of $\sigma_{\rm IP}(r)$ at $r \sim R_c$ and is relatively insensitive to the large-r behavior of $\sigma_{\rm IP}(r)$.

The intercept $\delta(\beta)$ will have a maximum at $\beta = 0$. Then, repeating the derivation of the Green's function (17) one can easily show that at large r,r' the Green's function of Eq. (39) has the behavior

$$K(\xi,r,r') \propto \frac{\exp(\Delta_{\rm IP}\xi)}{\sqrt{\xi}}\exp\left(-\frac{\mu_G^2(r-r')^2}{2\xi\delta''(0)}\right), \tag{41}$$

which is reminiscent of the familiar multiperipheral diffusion. Indeed, at large $r \gg 1/\mu_G$ a sort of the additive quark model is recovered, in which the (anti)quark of the dipole develops its own perturbative gluonic cloud, and the quark-quark scattering will be described by the multiperipheral exchange of massive vector mesons. The Green's function (28) shows the emergence of the Regge growth of the interaction radius in this limit. It also shows that the large-ξ behavior of solutions of our generalized BFKL equation in this region will be similar to solutions of the Schrödinger equation

$$\left[-\frac{\delta''(0)}{2\mu_G^2}\frac{\partial^2}{\partial r^2}+U(r)\right]\Phi=-\frac{\partial}{\partial\xi}\Phi=\varepsilon\Phi \tag{42}$$

with the potential $U(r)=-\delta(0)$, which is flat for $r>R_c$.

The scaling limit of Eq. (11) does not have localized solutions [see the eigenfunctions (13)]. An important observation is that Eq. (39) also does not have node-free localized solutions, which vanish at large r. Indeed, if such a solution had existed, then the l.h.s. of Eq. (39) would have vanished at $r\to\infty$. For the same reason, we can neglect $\sigma(r)$ and $\sigma(\rho_2)$ in the integrand of the r.h.s. of (39) and will be left with the positive-valued and r-independent contribution from $\sigma(\rho_1)$. This shows that (40) gives a complete set of solutions. Consequently, the BFKL equation thus generalized only has the continuous spectrum, and the partial-wave amplitudes only have the branching point singularity (cut) in the complex-j plane.

We wish to emphasize that none of the above conclusions change if $K_1(\mu_G r)$ is replaced by any function which vanishes sufficiently steeply at large r. The only condition is that it must have the short-distance $1/r$ behavior dictated by the $1/k^2$ ultraviolet behavior of the perturbative gluon propagator.

5.3. Massless gluons with running and freezing coupling

The second interesting case is of $R_c\to\infty$, i.e., the case of massless gluons, $\mu_G\to 0$, but with the running coupling which freezes, $\alpha_S(r)=\alpha_S^{(fr)}=\alpha_S(R_f)$, for finite $r\geqslant R_f$. In this case the scaling invariance of the kernel $\mathscr{K}$ is restored on the infinite semiaxis $\log r>\log R_c$, where the eigenfunctions $E_+(i\nu,\xi,r)$ are again essentially identical to the BFKL set (13), the spectrum of eigenvalues will evidently be continuous, the intercept Δ_{IP} will be given by the BFKL formula (15) with $\alpha_S=\alpha_S^{(fr)}$ and the partial waves of the scattering amplitude will have a cut in the j-plane identical to that for the original BFKL equation. Indeed, the corresponding "Schrödinger" Eq. (38) has a continuous spectrum starting from $\varepsilon=-\Delta(0)$, and this conclusion is evidently insensitive to the exact shape of the potential $V(z)$ at $z\lesssim z_f$. Here we agree with Ross *et al.*[11,14] and disagree with Lipatov,[3] who concluded that introduction of the running coupling is by itself sufficient for transformation of the continuous spectrum of the pomeron to a discrete one. Apparently, the origin of this conclusion is that Lipatov[3] restricted himself to a very special form of the solution at large r, rather than using the continuum solutions (40).

The continuation of the BFKL solutions (13) to the region of $z<z_f=\log R_f^2$ poses no problems. Let us start with the quasiclassical situation when $\alpha^{(fr)}\ll 1$, so that

$$\alpha_S(z)=\alpha_S(R_f)[1+(\beta_0/4\pi)\alpha_S(R_f)(z_f-z)]^{-1}$$

is a slow function of z. In this case the slowly varying running coupling can be factored out from the integrand of Eqs. (10) and (11). This suggests that to a crude approximation one may make a substitution of the fixed coupling α_S in Eq. (14) for the running coupling $\alpha_S(r)$. Consequently, Eq. (38) takes the form of the "Schrödinger" equation for a particle with the slowly varying mass

$$M(z)\sim\frac{1}{\Delta''(0)}\frac{\alpha_S(R_f)}{\alpha_S(r)} \tag{43}$$

in the potential

$$V(z)\sim-\Delta_{\mathrm{IP}}\frac{\alpha_S(r)}{\alpha_S(R_f)}, \tag{44}$$

which is slowly varying and monotonically decreasing in magnitude and flat, $V(z)=-\Delta_{\mathrm{IP}}$, for $z>z_f$. Evidently the solutions $E_+(i\nu,\xi,r)$ with $\Delta(i\nu)>0$, i.e., with negative energy ε, will have a subbarrier decrease at $z\to-\infty$, whereas the solutions with $\Delta(i\nu)<0$ will be continued to $z\ll z_f$ as plane waves. This suggests that the eigenfunction $\sigma_{\mathrm{IP}}(r)$ for the rightmost singularity will decrease at $r\to 0$ faster than the solution (18) $\propto r^1$ for the fixed-α_S scaling BFKL regime. The case of large values of the frozen coupling $\alpha_S^{(fr)}$ must be qualitatively the same.

In Sec. 4 we have discussed the conventional DLLA solution of the GLDAP equation, which has a limited domain of applicability. Besides this conventional DLLA solution, in the weak-coupling limit of $\alpha_S(r)\ll 1$ the GLDAP Eq. (24) has the new one-parametric family of solutions which have the Regge behavior $\propto\exp(\Delta\xi)$. It can best be described in terms of the gluon density

$$G(\xi,r)=xg(x,r)=\frac{3\sigma(\xi,r)}{\pi^2 r^2\alpha_S(r)}. \tag{45}$$

After we factor out $\alpha_S(r)$ from the kernel $\mathscr{K}$, which we shall justify *à posteriori*, our generalized BFKL equation (11) takes the form

$$\frac{\partial G(\xi,r)}{\partial\xi}=\frac{3}{2\pi^2}\int d^2\rho_1\left[\frac{\alpha_S(\rho_1)G(\xi,\rho_1)}{\rho_2^2}+\frac{\alpha_S(\rho_2)G(\xi,\rho_2)}{\rho_1^2}-\frac{r^2\alpha_S(r)G(\xi,r)}{\rho_1^2\rho_2^2}\right]. \tag{46}$$

À posteriori, we can show that the last term $\propto\alpha_S(r)G(\xi,r)$ can be neglected for $\alpha_S(r)\ll 1$. Then Eq. (47) takes the form

$$\frac{\partial G(\xi,r)}{\partial\xi}=\frac{4}{3}\int_0^{L(R,r)}dL(R,\rho)G(\xi,\rho), \tag{47}$$

which has the one-parametric family of small-r, large-$L(R,r)$ eigenfunctions

$$e_-(\gamma,\xi,r)=\exp[\gamma L(R,r)]\exp(\Delta\xi)=\left[\frac{1}{\alpha_S(r)}\right]^{\gamma}\exp(\Delta\xi), \tag{48}$$

where the exponent γ is related to the intercept Δ by

$$\gamma=\frac{4}{3\Delta}. \tag{49}$$

The corresponding dipole cross section equals

$$\sigma_-(\gamma,r)=r^2\left[\frac{1}{\alpha_S(r)}\right]^{\gamma-1}\exp(\Delta\xi). \tag{50}$$

In contrast to the conventional DLLA solution (28) which sums the leading powers $[L(R,r)\xi]^n$, our new solutions (48) and (50) do manifestly sum all powers $L^k(R,r)$. The accuracy of this solution can be understood by making use of (48) in Eq. (46): the neglected term $\propto\alpha_S(r)G(\xi,r)$ gives the $\propto\alpha_S(r)$ correction to the solution (48).

The small-r considerations alone do not fix the intercept Δ and the exponent γ, they are determined from the matching the solution $e_-(\gamma,\xi,r)$ with the large-r solution $E_+(i\nu,\xi,r)$.

5.4. The strong coupling freezes at $R_f \sim R_c$

This realistic case of greatest interest is a combination of the two previous cases. It is convenient to start from the region $r>R_c,R_f$. The only change from Eq. (39) will be that the running coupling α_S must be absorbed into the integrand

$$\sigma_{n+1}(r)=\frac{3}{\pi^3}\int d^2\rho_1\alpha_S(\rho_1)\mu_G^2K_1(\mu_G\rho_1)^2 \times[\sigma_n(\rho_1)+\sigma_n(\rho_2)-\sigma_n(r)]. \quad (51)$$

This equation has a continuum of solutions of the form (40) with the spectral parameter $-\infty<\beta<+\infty$, and its large-r Green's function and the corresponding Schrödinger operator will be similar to (41) and (42), respectively. Therefore, Eq. (51) has a continuous spectrum and the scattering amplitude will have a cut in the complex j-plane. Continuation of the large-r solutions to small r is no different from that discussed in Subsec. 5.3. Evidently, the intercept Δ_{IP} of the rightmost singularity in the j-plane corresponds to the eigenvalue $\delta(\beta)$ with $\beta=0$, $\Delta_{\mathrm{IP}}=\delta(0)$, as the corresponding eigenfunction does not have a node. For this solution $\delta_{\mathrm{IP}}(\xi,r)=\mathrm{const}$ vs r at large r, and decreases faster than $\propto r$ at $r\to 0$. From Eq. (51) it is obvious, that the intercept Δ_{IP} is mostly controlled by the contribution from $r\sim R_c$. Also, repeating the considerations of Subsec. 5.1, we can exclude the node-free localized solutions of Eq. (51) with $\sigma(r)$ vanishing at large r. This shows that our generalized BFKL equation only has a continuous spectrum and the partial-wave amplitudes only have a cut in the complex j-plane.

5.5. Can the pomeron have a discrete spectrum?

The discrete spectrum of the pomeron, i.e., generation of isolated poles in the complex-j plane, occurs when localized solutions of the generalized BFKL equation exist. The above elimination of localized solutions is rigorous in the framework of our minimal infrared regularization. Technically, it is based on the kernel $\mathscr{K}$ being finite at $r\to\infty$ [see Eqs. (39) and (51)], which gives rise to $\sigma(r)\sim\mathrm{const}$ for $r>R_c$ and to a continuum of solutions of the form (40). The interaction picture which emerges at $r>R_c$ has much intuitive appeal: each well separated quark of the beam (target) dipole develops a perturbative gluonic cloud of its own, and a sort of additive quark model is recovered. At first sight, the localized solutions with the vanishing perturbative total cross section for color dipoles of large size, $\sigma(r)\to 0$ at $r\to\infty$, look quite unphysical.

Here we we wish to present the qualitative arguments in favor of the possibility of localized solutions. The plausible scenario for the discrete spectrum of the pomeron is as follows: The kernel $\mathscr{K}$ is proportional to the probability for radiation of perturbative gluons [see Eq. (9)]. When the quarks of the color dipole are a distance $r\gg R_c$ apart, the nonperturbative color fields stretched between the quarks may strongly modify the vacuum and suppress the perturbative gluonic fluctuations on the nonperturbative background in the vicinity of quarks. Because the nonperturbative background fields are strongly anisotropic, this suppression of the perturbative gluonic fluctuations also will be anisotropic. However, to a very crude approximation this suppression can be modeled by the decrease with increasing r of the effective (nonlocal) perturbative coupling $\alpha_S(r,\rho)$ and/or the increase of μ_G with increasing r, resulting in the decrease of the kernel $\mathscr{K}$ with increasing r. In terms of the Schrödinger Eq. (42) this amounts to a rise of the potential $U(r)$ toward large r. [One can draw a useful analogy with the asymptotic-freedom decrease of $\alpha_S(r)$ and the related rise of $V(z)$ [Eq. (44)] in the Schrödinger Eq. (38).] As a natural scale at which such a suppression of the perturbative fluctuations can take place one can think of the confinement radius R_{conf}, which is of the order of the diameter of hadrons, $R_{\mathrm{conf}}\sim 1-2F$. Evidently, the energy ε of the lowest state will be higher than the bottom of the potential well, so that the intercept Δ_{IP} of the rightmost singularity will be lowered than in the case of the minimal regularization. If with increasing r the potential $U(r)$ flattens at the still negative value $U(\infty)=-\Delta_c$, then the Schrödinger Eq. (29) will have a continuous spectrum starting with $\varepsilon=-\Delta_c$, and in the complex j-plane there will be a cut from $j=1+\Delta_c$ to $j=-\infty$ and a certain number of isolated poles to the right of the cut, at $1+\Delta_c<j\leqslant 1+\Delta_{\mathrm{IP}}$. If $U(\infty)>0$, then the cut in the complex j-plane will start at $j=1$.

Although the above considerations are very qualitative ones, we regard them as giving a sound correlation between the discrete spectrum of the pomeron and the nonperturative suppression of the perturbative gluonic fluctuations in large color dipoles. (We do not suggest a dynamical mechanism for such a suppression, though.) In Subsec. 5.3 we explained why we disagree with Lipatov's conclusion[3] that the running coupling does by itself generate the discret spectrum of the pomeron (see Subsec. 5.3). Ross and Hancock[11] try to eliminate the contribution of the infrared region by a k^2-cutoff in the asymmetric form of the BFKL Eq. (22) and find a discrete spectrum of the pomeron for several models of the nonperturbative gluon propagator. The significance of their findings is not clear to us, since the Hancock-Ross procedure violates the symmetry of the cutoff of gluon propagators and its consistency with gauge invariance is questionable (for a critique of this procedure see Sec. 3). For this reason the correspondance between the Ross-Hancock cutoff and the above nonperturbative suppression of the perturbative gluon fluctuations is not evident to us.

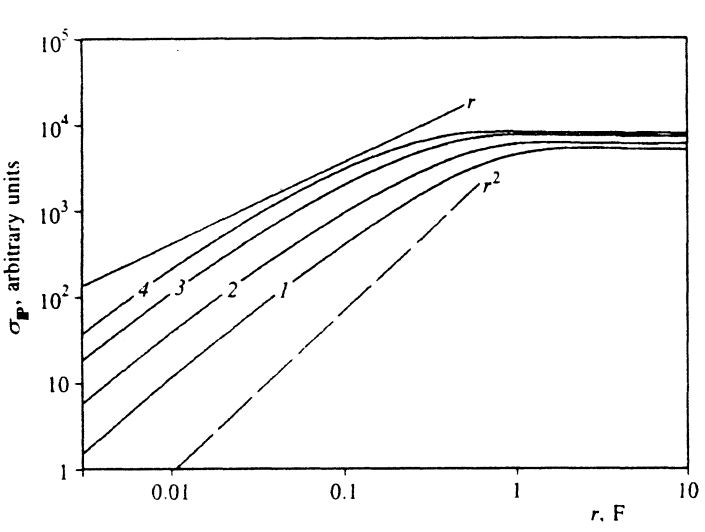

FIG. 1. The pomeron dipole cross section $\sigma_{IP}(r)$ for different values of μ_G: *1*—0.3 GeV, *2*—0.5 GeV, *3*—0.75 GeV, 4—1.0 GeV. The straight lines show the r and r^2 behavior.

6. THE EVALUATION OF Δ_{IP} AND THE POMERON DIPOLE CROSS SECTION

Equations (10) and (11) can not be solved analytically for finite R_c and with the running coupling, and we resort to the numerical analysis. We study the large-ξ behavior of numerical solutions of Eq. (11) and verify that $\sigma(\xi,r)$ has the same asymptotic behavior $\sigma(\xi,r) \Rightarrow \sigma_{IP}(r)\exp(\Delta_{IP}\xi)$ (within the overall normalization) irrespective of the boundary condition at $\xi=0$. Namely, we compute the effective intercept

$$\Delta_{eff}(\xi,r)=\partial \log \sigma(\xi,r)/\partial\xi \tag{52}$$

and check that at large ξ the effective intercept $\Delta_{eff}(\xi,r)$ tends to the same limiting value Δ_{IP} for all r. Flattening of $\Delta_{eff}(\xi,r)$ as a function of r and as a function of ξ takes place at about the same value of ξ, and in all the cases the flattening was good to a few parts in a thousand. In Fig. 1 we present the eigenfunction $\sigma_{IP}(r)$ for several values of the gluon correlation radius $R_c=1/\mu_G$ [we keep the same running strong coupling $\alpha_S(r)$ which freezes at $\alpha_S^{(fr)}=0.8$]. As anticipated above, $\sigma_{IP}(r)$ flattens at large r and decreases toward small r faster than the BFKL solution (18), but slower that r^2.

The physical interaction picture behind this emergence of the factorizing r and ξ dependences of the asymptotic cross section is as follows: Consider, for instance, the interaction of two small-sized dipoles $r_A, r_B \ll R_c$. Radiation of perturbative gluons by such dipoles is supprressed by the color cancellations and by the small coupling $\alpha_S(r)$. However, the perturbative gluons start sticking out of the initially small dipoles at a distance $r\sim R_c$. Consequently, after few steps of radiation and/or after few units in ξ the gluonic cloud with size $\sim R_c$ builds up, the evolution of which is controlled by $\alpha_S(R_c)\approx\alpha_S^{(fr)}$, and whose interaction properties do not depend on the size of the initial beam and target dipoles. The size of the beam and target dipoles only controls the rate of the evolution of the limiting gluonic cloud (for more discussion on this point see below).

In Fig. 2 we present the intercept Δ_{IP} for few values of μ_G=0.3, 0.5, 0.75, 1.0 GeV. As we have emphasized above, this intercept is controlled by interactions of the semiperturbative gluons at transverse distances $r\sim R_c$, where the strong coupling is rather large, $\alpha_S(R_c)\approx\alpha_S^{(fr)}$. For comparison, with $\alpha_S=0.8$ the BFKL formula (15) gives $\Delta_{IP}(\text{BFKL})=2.12$. We recall that the BFKL formula is only valid in the scaling limit of $R_c\to\infty$ and obviously overestimates the intercept for the case of finite R_c. In the literature one often cites the CK lower bound[9]

$$\Delta_{IP}>\frac{3.6}{\pi}\alpha_S^{(fr)} \tag{53}$$

This bound was derived in the model with the CK sharp cutoff $k^2>k_0^2$ in the asymmetric form of the BFKL Eq. (22) with massless gluons, $m^2=0$. For a closer comparison with the CK bound we substitute $\alpha_S^{(fr)}$ in Eq. (53) for $\min\{\alpha_S(\mu_G^2),0.8\}$. The resulting bound is shown in Fig. 2 and is not supported by our results. The significance of the CK bound is questionable though, since the derivation[9] of the CK bound is plagued by violations of the symmetry of the BFKL equation; for a critique see Sec. 3.

In terms of the exponent γ of the small-r solutions (48), we have $\gamma-1=1.19, 1.81, 2.33, 2.70$ at μ_G=0.3, 0.5, 0.75, 1.0 GeV, respectively. The smaller μ_G is the smaller is $\gamma-1$ and the steeper is the decrease of $\sigma_{IP}(r)$ at small r, in

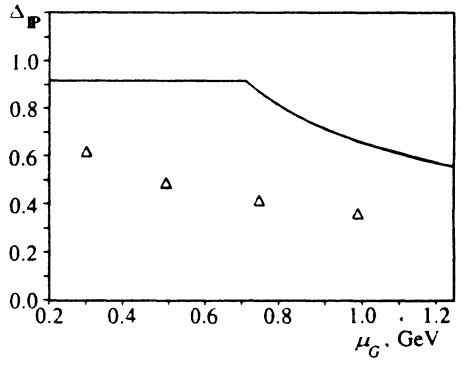

FIG. 2. The intercept Δ_{IP} for μ_G=0.3, 0.5, 0.75, 1.0 GeV (shown by triangles). The solid curve shows the Collins–Kwiecinski lower bound (53).

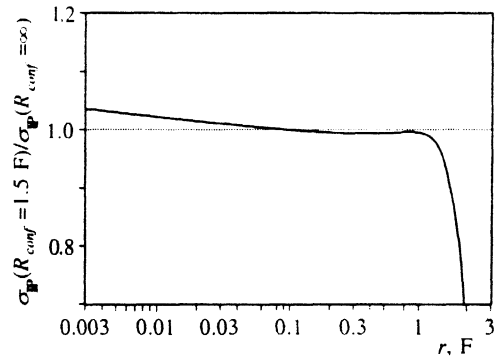

FIG. 3. The ratio of the pomeron dipole cross section with the cutoff (54) of the large-r contribution to the pomeron dipole cross section without the cutoff. The cutoff radius is $R_{\rm conf}=1.5$ F and the gluon correlation radius is $R_c=0.275$ F.

agreement with the results shown in Fig. 1 (for more discussion on the relevance of solutions (48) to $\sigma_{\rm IP}(r)$ see below, Subsec. 7.3).

In Subsec. 5.5 we discussed the possibility of generating the discrete spectrum of the pomeron via the (purely hypothetical) mechanism of the nonperturbative suppression of perturbative gluonic fluctuations in color dipoles of large size. Such a suppresion must lower the intercept of the pomeron. For a crude evaluation of the possible effect, we introduce in front of the kernel $\mathscr{K}$ the suppression factor

$$\mathscr{K}\Rightarrow\frac{2}{1+\exp[(r-R_{\rm conf})^2\theta(r-R_{\rm conf})/d^2]}\mathscr{K}. \quad (54)$$

We consider the case of $\mu_G=0.75$ GeV, i.e., $R_c=0.275$ F, and take $d=0.5$ F and $R_{\rm conf}=1.5$ F, i.e., impose strong suppression of the perturbative gluonic fluctuations already at r of the order of the diameter of hadrons. In terms of the Schrödinger Eq. (42) this steep suppression factor corresponds to an abrupt rise of the potential $U(r)$ at $r\approx R_{\rm conf}$. All this serves to enhance the discussed effect. We find a negligible change, less than one percent of $\Delta_{\rm IP}$ with respect to the case of $R_{\rm conf}=\infty$. Such a small effect could have easily been anticipated: the intercept $\Delta_{\rm IP}$ is primarily sensitive to the behavior of $\sigma_{\rm IP}(r)$ at $r\sim R_c$, and although we have enforced very dramatic suppression of the perturbative gluonic fluctuations, the effect on the intercept is small because of the strong inequality $R_c\ll R_{\rm conf}$. This interpretation is confirmed by Fig. 3, in which we show the ratio of $\sigma_{\rm IP}(R_{\rm conf}=1.5F,r)$ to $\sigma_{\rm IP}(R_{\rm conf}=\infty,r)$, and this ratio is essentially unity up to $r\sim 5R_c\approx 1.4$ F. This result strongly suggests, that the intercept of the pomeron is a semiperturbative quantity, insensitive to the truly large-distance effects.

In this paper we only concentrate on the rightmost singularity, and we do not evaluate the gap between the poles in the discrete spectrum. We only comment that the convergence of $\Delta_{\rm eff}(\xi,r)$ to the limiting value $\Delta_{\rm IP}$ becomes faster when the large-r cutoff (54) is imposed, which suggests that the rightmost singularity is a pole separated from other singularities by a gap.

Consequently, with all the due reservations on the large-distance QCD, we conclude that the intercept of the perturbative QCD pomeron is significantly higher than the effective intercept $\Delta_{\rm IP}(hN)\sim 0.1$ as given by the phenomenology of hadronic scattering.[15] The plausible scenario, suggested by the observed slow rise of the hadronic cross sections, is that the exchange by perturbative gluons is only a small part of $\sigma_{\rm tot}(hN)$ at moderate energies (Ref. 5; for an early discussion of this scenario see Ref. 16). The detailed phenomenology of the hadronic cross sections will be presented elsewhere.

7. THE GLDAP AND BFKL EVOLUTIONS IN DEEP INELASTIC SCATTERING

7.1. Deep inelastic scattering and the dipole cross section

The representation (3) is universal and also applies to deep inelastic scattering.[4,6] The wave functions of the transverse (T) and longitudinal (L) virtual photon of virtuality Q^2 were derived in Ref. 6 and read

$$|\Psi_T(z,r)|^2=\frac{6\alpha_{em}}{(2\pi)^2}\sum_1^{N_f}Z_f^2\{[z^2+(1-z)^2]\varepsilon^2K_1^2(\varepsilon r)+m_f^2K_0^2(\varepsilon r)\}, \quad (55)$$

$$|\Psi_L(z,r)|^2=\frac{6\alpha_{em}}{(2\pi)^2}\sum_1^{N_f}4Z_f^2Q^2z^2(1-z)^2K_0^2(\varepsilon r), \quad (56)$$

where

$$\varepsilon^2=z(1-z)Q^2+m_f^2. \quad (57)$$

In Eqs. (55)–(57) m_f is the quark mass and z is the Sudakov variable, i.e., the fraction of photon's lightcone momentum q_- carried by one of the quarks of the pair ($0<z<1$). Then

$$\sigma_{T,L}(\gamma^*N,\xi,Q^2)=\int_0^1 dz\int d^2r|\Psi_{T,L}(z,r)|^2\sigma(\xi,r), \quad (58)$$

and the structure function is calculated as

$$F_2(\xi,Q^2)=\frac{Q^2}{4\pi^2\alpha_{em}}[\sigma_T(\gamma^*N,\xi,Q^2)+\sigma_L(\gamma^*N,\xi,Q^2)]. \quad (59)$$

Making use of the properties of the modified Bessel functions, after the z-integration one can write

$$\sigma_T(\gamma^*N,\xi,Q^2)=\int_0^1 dz\int d^2r|\Psi_T(z,r)|^2\sigma(\xi,r)\propto\frac{1}{Q^2}\int_{1/Q^2}^{1/m_f^2}\frac{dr^2}{r^2}\frac{\sigma(\xi,r)}{r^2}. \quad (60)$$

Notice that the factor $1/Q^2$ in Eq. (60), which provides the Bjorken scaling, comes from the probability of having a $q\bar{q}$ fluctuation of the highly virtual photon. The ratio $\sigma(\xi,r)/r^2$ is a relatively smooth function of r, which slowly

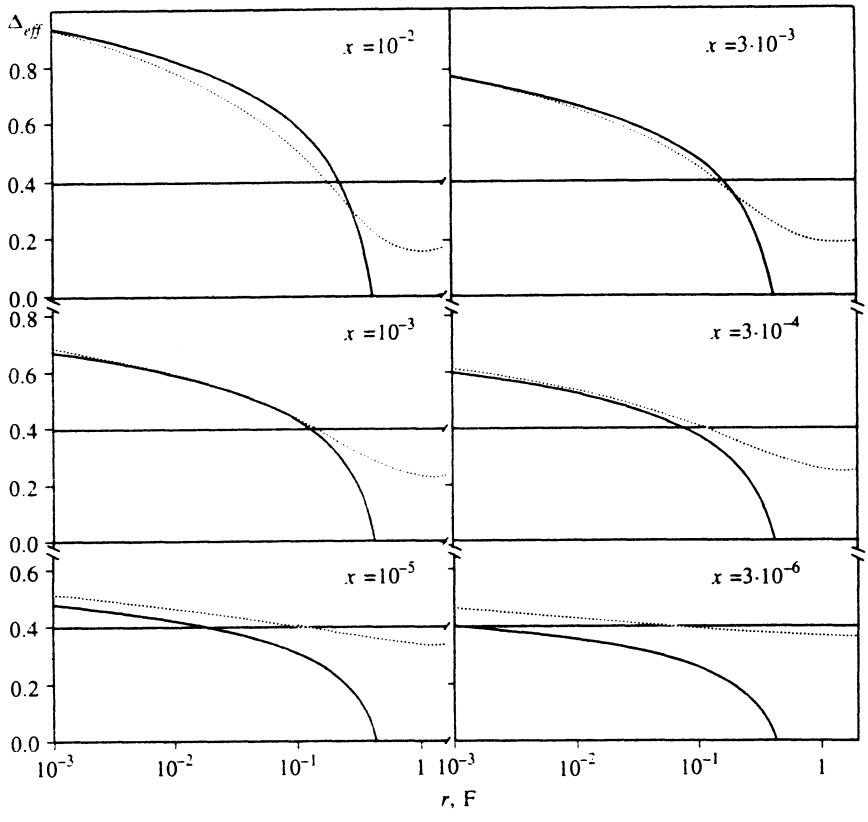

FIG. 4. Comparison of effective intercepts of the DLLA solution (64) to the GLDAP evolution (solid line) and of the solution of our BFKL equation (point line). Both solutions start with the same dipole cross section at $x=3\cdot10^{-2}$. The pomeron intercept $\Delta_{IP}=0.4$ is shown by the horizontal line.

rises toward small r. For the conventional DLLA behavior of $\sigma(\xi,r)$ see Eqs. (25) and (28); for the weak-coupling solution of our generalized BFKL equation see Eq. (50). Therefore, for the semiquantitative understanding of the transition from the GLDAP to the BFKL evolution we can concentrate on the r and ξ dependence of $\sigma(\xi,r)$.

7.2. The transition between the BFKL and DDLA regimes

One usually discusses the low-x behavior of structure functions in terms of the DLLA solution of the GLDAP evolution equations. In Sec. 4 we already commented on the breaking of DLLA at large $\xi=\log(x_0/x)$. Here we wish to concentrate on a comparison of the ξ-dependence of the perturbative GLDAP and BFKL solutions for $\sigma(\xi,r)$. The question of whether there is a strong, experimentally observable, difference between the BFKL and GLDAP evolutions, has been discussed in the literature for quite a time (Ref. 17 and references therein).

The DLLA solution to GLDAP evolution (28) gives the effective intercept

$$\Delta_{\mathrm{DDLA}}(\xi,r)=\frac{\partial}{\partial\xi}\left[2\sqrt{\eta}-\frac{1}{2}\log\xi\right]=\frac{4}{3}L(R,r)\left[\frac{1}{\sqrt{\eta}}-\frac{1}{2\eta}\right], \tag{61}$$

which must hold at $\eta\gtrsim1$ and moderately large $\xi\gtrsim1$. The DLLA intercept (61) vanishes at large ξ. On the other hand, in the BFKL regime the effective intercept (52) tends to Δ_{IP} irrespective of the radius r. This suggests a practical criterion: the DLLA approximation breaks at such values of $\xi=\xi_c(r)$, when $\Delta_{\mathrm{DLLA}}(\xi,r)$ becomes smaller than Δ_{IP}:

$$\Delta_{\mathrm{DLLA}}(\xi_c(r),r)\leqslant\Delta_{IP}. \tag{62}$$

Notice that since in expansion (28) the saddle point corresponds to $n\sim\sqrt{\eta}$, this criterion when combined with the effective intercept (61) essentially coincides with the DLLA breaking estimate (29).

For a meaningful comparison of the GLDAP and BFKL evolutions, we must take identical initial conditions. For the sake of definiteness we take $R_c=0.275$ F and consider scattering on the proton target, so that our initial condition for Eq. (11) is given by

$$\sigma(\xi=0,r)=\frac{3}{2}\int d^2R_{12}|\Psi_p(R_{12})|^2\sigma_0(R_{12},r), \tag{63}$$

where R_{12} is the separation of quarks "1" and "2" in the proton (for the details see Ref. 6). Since the DLLA asymptotic form (28) holds for $\xi\gtrsim1$, we shall consider the cross section (63) as a result of the GLDAP evolution by ξ_0 units from a lower energy, i.e., we take for the DLLA solution

$$\sigma_{\mathrm{DLLA}}(\xi,r)=\sigma(0,r)\sqrt{\frac{\xi_0}{\xi_0+\xi}}\times\exp\left[2\sqrt{\frac{4}{3}L(R_f,r)}\left(\sqrt{\xi_0+\xi}-\sqrt{\xi_0}\right)\right]. \tag{64}$$

It satisfies $\sigma_{\mathrm{DLLA}}(\xi=0,r)=\sigma(0,r)$ by construction, and we use it to evaluate the DLLA intercept in Eq. (61). The

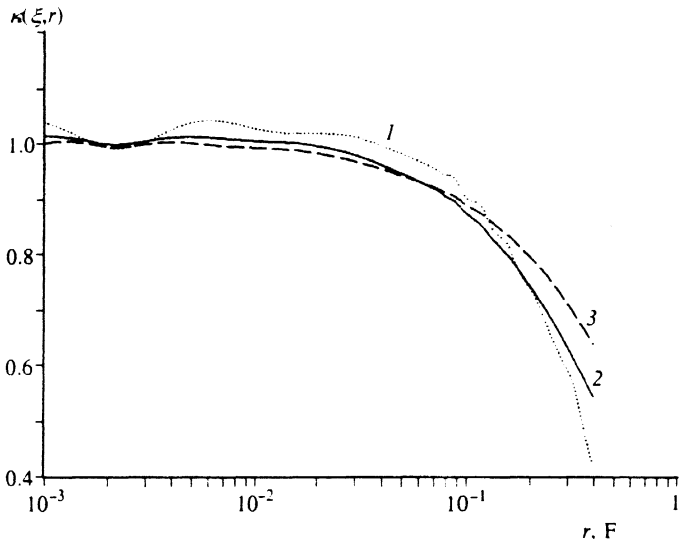

FIG. 5. Test of the DLLA identity for the solution of our generalized BFKL equation: *1*—$x=10^{-2}$, *2*—$x=3\cdot10^{-4}$, *3*—$x=3\cdot10^{-6}$. The gluon correlation radius is $R_c=0.275$F.

same $\sigma_0(r)$ is taken for the boundary condition for the BFKL Eq. (11). We assume this boundary condition to correspond to $x=x_0\approx 3\cdot 10^{-2}$.

Notice, that Eq. (25), the leading-logarithm formula, defines $L(R_f,r)$ up to an additive constant $c\lesssim 1$, which depends on the detailed form of the initial condition for ther GLDAP evolution, but which can be neglected in the DLLA limit of $L(R_f,r)\gg 1$. We compute $\Delta_{\text{eff}}(\xi=0,r)$ from our BFKL Eq. (11) and make the readjustment

$$L(R_f,r)\Rightarrow\log\left[\frac{\alpha_S^{(fr)}}{\alpha_S(r)}\right]+c \tag{65}$$

such that $\Delta_{\text{DLLA}}(\xi=0,r)$ of Eq. (61) gives a good approximation of $\Delta_{\text{eff}}(\xi=0,r)$ at small r. With $\xi_0=1.25$ this is achieved by taking $c\approx 0.05$.

The results of such a comparison of the BFKL and GLDAP evolutions are shown in Fig. 4. At $\xi=\log(x_0/x)\sim 1$, the DLLA and BFKL effective intercepts are both smaller than Δ_{IP} at $r\gtrsim 0.2$F and are larger than Δ_{IP} at smaller r. The good agreement of the BFKL and DLLA effective intercepts at small r is not surprising, since our generalized BFKL Eq. (11) has the GLDAP equation as a limiting case at small r (also see a discussion in Ref. 5). The ξ-evolution of the DLLA and BFKL effective intercepts is very much different, though: The BFKL effective intercept starts flattening as a function of r and tends to Δ_{IP}, rising at large r and decreasing at small r. In the opposite to that, the DLLA intercept monotonically decreases with ξ at all r, until the GLDAP breaking (62) takes place.

The boundary between the BFKL and DLLA regimes is given by our Eq. (32). The intercept Δ_{IP} is numerically small, $\Delta_{\text{IP}}=0.4$ at $\mu_G=0.75$, and the large numerical factor

$$\frac{4}{3\Delta_{\text{IP}}^2}\approx 8 \tag{66}$$

emerges in the r.h.s. of Eq. (32). Consequently, the DLLA-to-GLDAP evolution, and the GLDAP evolution itself, may remain numerically viable in quite a broad range of ξ, relevant to the kinematical range of HERA.

Closer inspection of Fig. 4 reveals a certain regularity: $\Delta_{\text{DLLA}}(\xi,r)$ decreases with ξ faster than $\Delta_{\text{eff}}(\xi,r)$, and the rate of the divergence is higher the larger the radius r. Hence, we look at the combined r and ξ dependence of $\sigma(\xi,r)$.

7.3. Testing the DLLA identity for the gluon distribution

In the DLLA, the gluon structure function $G(\xi,r)$ satisfies the equation (we consider $N_f=3$ active flavors)

$$\kappa(\xi,r)=\frac{3}{4}\frac{1}{G(\xi,r)}\frac{\partial^2 G(\xi,r)}{\partial\xi\partial L(R,r)}=1. \tag{67}$$

We shall refer to the equality $\kappa(\xi,r)=1$ as the DLLA identity. One can easily evaluate $\kappa(\xi,r)$ for the experimentally measured gluon distributions, and it is tempting to consider the departure from the DLLA identity as a measure of the accuracy of the GLDAP evolution. In this section we apply such a test of the DLLA identity to the above solution of our generalized BFKL equation (11) subject to the boundary condition (63).

The results of such a test are shown in Fig. 5. We find that our BFKL solution produces $\kappa(\xi,r)\approx 1$ in a very broad range of ξ and r of practical interest. Remarkably, the DLLA identity holds to within 20–30% even at large r, up to $r^2\lesssim 1/2\,R_c^2$, and to a few percent accuracy at $r\lesssim 1/3\,R_c$. Notice the somewhat oscillatory r-dependence of the $\Delta_{\text{eff}}(\xi,r)$ for our BFKL solution. These oscillations die out at large ξ. They have an origin in the presence of harmonics with large $|\nu|$ and/or large $|\beta|$ in the expansion of the boundary condition (63) in terms of eigenfunctions of the kernel $\mathscr{K}$ (for instance, see Eqs. (16) and (17). These eigenfunctions give the oscillating contribution to $\sigma(\xi,r)$, see Eqs. (16) and (40). We have checked

that the DLLA identity $\kappa(\xi,r)=1$ is satisfied by solutions of our generalized BFKL equation to a very good accuracy in a broad range of R_c and $\Lambda_{\rm QCD}$.

The obvious conclusion from this observation is that the DLLA solution (28), which is only valid at moderate values of ξ, evolves at larger ξ into our new solution (50). These new solutions satisfy our BFKL equation to $\sim\alpha_S(r)$ and also satisfy the DLLA identity, although it was not obvious that $\sigma_{\rm IP}(\xi,r)$ necessarily belongs to this new family of GLDAP/BFKL solutions (50). The exponent γ is uniquely fixed by the pomeron intercept $\Delta_{\rm IP}$ via Eq. (49). We have checked that the pomeron dipole cross sections $\sigma_{\rm IP}(r)$ shown in Fig. 1 do indeed accurately satisfy the property

$$\frac{\sigma_{\rm IP}(r)}{r^2}\,[\alpha_S(r)]^{\gamma-1}=\text{const} \tag{68}$$

up to $r\lesssim 1/2R_c$.

This observation shows that, as matter of fact, there is no real clash between the GLDAP and BFKL evolutions if $\alpha_S(r)$ is running. To his end, an important point to note is that the discussion of the BFKL effects in the current literature concentrates upon the fixed $-\alpha_S$ approximation (for a review and references see Ref. 18). We have found that the effect of the running coupling constant is quite substantial. Firstly, the pomeron cross section (50) dramatically differs from the BFKL scaling solution $\propto r$ at fixed α_S (see also Fig. 1). Secondly, one can define the counterpart of the DLLA identity for fixed α_S too, making the substitution

$$L(R,r)=\frac{\beta_0}{4\pi}\int_{r^2}^{R^2}\frac{d\rho^2}{\rho^2}\,\alpha_S(\rho)\Rightarrow\frac{\beta_0}{4\pi}\,\alpha_S\log\left(\frac{R^2}{r^2}\right). \tag{69}$$

Then, the BFKL scaling pomeron solution (18) gives

$$\kappa=2\log 2, \tag{70}$$

which also emphasizes the dramatic difference between the cases of the fixed and running strong coupling. Hence matching the fixed-α_S BFKL regime at small x with the GLDAP regime at larger x is doomed to inconsistencies, and such considerations are not appropriate for the phenomenology of deep-inelastic scattering.

One interesting feature of the DLLA identity is worthy of mention. We have calculated $\kappa(\xi,r)$ for solutions of our generalized BFKL equation for various boundary conditions, including the completely unphysical $\sigma(\xi=0,r)$ which has the form of two Gaussian peaks with large spacing in r. Because of the diffusion in the radius r, the dip between the two Gaussians fills in very rapidly. As soon as such a $\sigma(\xi,r)$ becomes a relatively smooth function of r, this is followed by a rapid approach of $\kappa(\xi,r)$ to unity. We find $\lesssim$10–15% departure of $\kappa(\xi,r)$ from unity even for $\xi\gtrsim 2-3$ and $\lesssim 5\%$ departure for $\xi\gtrsim 5$. This fulfillment of the DLLA identity takes place when $\sigma(\xi,r)$ has the r-dependence still very different from the typical DLLA solution and/or the asymptotic pomeron cross section $\sigma_{\rm IP}(r)$. One plausible interpretation of this observation is that, apart from the solution for the rightmost singularity at $j=1+\Delta_{\rm IP}$, the (approximate) DLLA identity holds for other solutions in a relatively broad range of $j\lesssim 1+\Delta_{\rm IP}$. The corresponding analysis goes beyond the scope of the present paper.

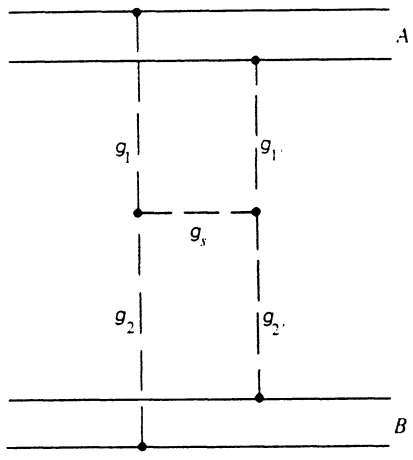

FIG. 6. One of the diagrams of the driving term of the rising dipole cross section.

We conclude this section with a prediction of the universal scaling violation at asymptotically large ξ. Namely, making use of (50) in Eq. (60), we obtain

$$F_{2p}(x,Q^2)\propto\left[\frac{1}{\alpha_S(q^2)}\right]^{4/3\Delta_{\rm IP}}\left(\frac{1}{x}\right)^{\Delta_{\rm IP}}. \tag{71}$$

The results of Fig. 4 suggest, though, that the onset of this universal scaling violation is well beyond the kinematical range of the HERA experiments.

8. THE BEAM-TARGET SYMMETRY AND THE BOUNDARY CONDITION

In the above discussion we have suppressed the target size variables r_B but, evidently, it is the generalized energy-dependent dipole–dipole cross section $\sigma(\xi,\mathbf{r}_A,\mathbf{r}_B)$ which emerges as the fundamental quantity of the lightcone s-channel approach to the diffractive scattering. The lowest-order dipole–dipole cross section has the obvious beam–target symmetry property $\sigma_0(\mathbf{r}_A,\mathbf{r}_B)=\sigma_0(\mathbf{r}_B,\mathbf{r}_A)$. This beam–target symmetry is but a requirement of the Lorentz-invariance and one has to have it extended to all energies. Thus, the beam–target symmetry emerges as an important constraint on the admissible boundary condition for the BFKL equation. In the derivation of our generalized BFKL equation we have treated the s-channel gluon g_s of Fig. 6 as belonging to the beam–dipole A. The gluon-induced correction to the total cross section was reinterpreted in terms of the generalized dipole cross section $\sigma(\xi,\mathbf{r}_A,\mathbf{r}_B)$ [see Eq. (9)]. Alternatively, we could have treated the same s-channel gluon g_s as belonging to the target dipole, and the result would have been the same. The two descriptions differ in that in the former the perturbative t-channel gluons g_1 and $g_{1'}$ enter the kernel $\mathcal{K}_A$, which we label with the subscript A as it acts on the beam variable r_A of the dipole–dipole cross section $\sigma(\xi,\mathbf{r}_A,\mathbf{r}_B)$, whereas the gluons g_2 and $g_{2'}$ are the exchanged gluons in

the dipole-dipole cross section (1). In the latter description $g_2,g_{2'}$ enter the kernel $\mathscr{K}_B$, which now acts on the target variable r_B of the dipole–dipole cross section $\sigma(\xi,\mathbf{r}_A,\mathbf{r}_B)$, and $g_1,g_{1'}$ will become the exchanged gluons in the input dipole-dipole cross section. The beam-target symmetry constraint essentially implies, that the boundary condition for the BFKL evolution must be calculable in the same perturbation theory as the one used to construct the generalized BFKL kernel $\mathscr{K}$ Eq. (10). [To this end we recall that the $K_1(x)$ in the kernel $\mathscr{K}$ is precisely the derivative of the gluon propagator (correlation function) $K_0(x)$.] This kernel–cross section relationship is crucial for having the beam–target symmetry, which will be violated with the arbitrary choice of the boundary condition for the dipole–dipole cross section $\sigma(\xi=0,\mathbf{r}_A,\mathbf{r}_B)$.

9. RESTORATION OF FACTORIZATION AT ASYMPTOTIC ENERGIES

It is well known that in the conventional Regge theory the isolated poles in the complex-j plane give rise to factorizing scattering amplitudes. Even if the factorization holds for separate singularities in the j-plane, the scattering amplitude, which is a sum of contributions from many close-by singularities, does not factorize. For instance, the lowest order dipole–dipole cross section (1) manifestly breaks the factorization relation. It is interesting to notice that the factorization of the total cross sections restores at asymptotic energies.

Specifically, for the rightmost singularity in the j-plane the beam–target symmetric dipole–dipole total cross section will have the factorized form

$$\sigma_{\mathrm{IP}}(\xi,\mathbf{r}_A,\mathbf{r}_B)=\sigma_{\mathrm{IP}}(r_A)\sigma_{\mathrm{IP}}(r_B)\exp(\xi\Delta_{\mathrm{IP}}). \tag{72}$$

By virtue of Eq. (2) this implies that at asymptotic energies

$$\sigma_{\mathrm{tot}}(AB)\propto\left[\int dz_A d^2r_A\left|\Psi(z_A,\mathbf{r}_A)\right|^2\sigma_{\mathrm{IP}}(r_A)\right]\times\left[\int dz_B d^2r_B\left|\Psi(z_B,\mathbf{r}_B)\right|^2\sigma_{\mathrm{IP}}(r_B)\right]\exp(\Delta_{\mathrm{IP}}\xi), \tag{73}$$

which has the manifestly factorized form. From the point of view of the phenomenology of the total cross sections, this factorization will be broken by the unitarization corrections needed to tame too rapid a rise of the perturbative bare pomeron cross section. The above universal scaling violation in deep inelastic scattering is a particular case of this factorization restoration.

10. MEASURING THE BFKL POMERON AT HERA

The experimental determination of the pomeron intercept Δ_{IP} requires isolation of the BFKL pomeron cross section, which is not an easy task because of the close similarity of the BFKL and GLDAP solutions, discusssed in detail in Sec. 7. The GLDAP evolution is a special limiting case of the BFKL evolution. Not every solution of the BFKL equation satisfies the GLDAP evolution and the DLLA identity. Our remarkable finding is that the small-r pomeron cross section (50), which is a solution of the BFKL equation, satisfies the GLDAP evolution equation to within correction terms $\sim\alpha_S(r)$. Consequently, one may expect that GLDAP evolution with the proper boundary condition can be a good approximation to the BFKL evolution. The GLDAP considerations can not by themselves fix this boundary condition, though. Inspection of Fig. 4 shows that the DLLA and BFKL effective intercepts are close to each other and to the Δ_{IP} in a broad range of x of practical interest at

$$r\approx r_0=(0.4-0.5)R_c. \tag{74}$$

Consequently, choosing boundary condition $G(\xi,r_0)\propto x^{-\Delta_{\mathrm{IP}}}$ at $r\approx r_0$, one will obtain the GLDAP solutions, which for $r\lesssim r_0$ will be indistinguishable for all practical purposes from the BFKL solution. Eq. (60) shows that the proton structure function receives contributions from the broad range of r in which the effective intercept $\Delta_{\mathrm{eff}}(r)$ is substantially different from Δ_{IP}. For this reason, studying the x-dependence of $F_2(x,Q^2)$ is not suitable for accurate determination of the pomeron intercept.

Figure 4 suggests that by zooming in to $r\approx 0.15-0.2$ F one can determine the pomeron intercept Δ_{IP} even at the moderately large $1/x$ of the HERA experiments. This can be achieved by measuring either the longitudinal structure function $F_L(x,Q^2)$ or the scaling violations in the transverse structure function $\partial F_T(x,Q^2)/\partial\log(Q^2)$. Making use of the wave functions (55) and (56) one can easily show that these quantities are local probes of $\sigma(\xi,r)$ at

$$r^2\approx\frac{B}{Q^2}, \tag{75}$$

where for the longitudinal and transverse structure functions we have $B_L\approx 12$ and $B_T\approx 5$. Consequently, experimentally Δ_{IP} can best be estimated as

$$\Delta_{\mathrm{IP}}=-\frac{\partial\log F_L(x,Q^2)}{\partial\log x} \tag{76}$$

at $Q^2=Q_L^2\approx$ 12–25 GeV^2 and/or

$$\Delta_{\mathrm{IP}}=-\frac{1}{F_T(x,Q^2)}\frac{\partial^2\log F_T(x,Q^2)}{\partial\log x\partial\log Q^2} \tag{77}$$

at $Q^2=Q_T^2\approx$ 5–8 GeV^2. Our prediction is that these derivatives must be x-independent already starting with $x\lesssim 10^{-2}$. The above difference between Q_L^2 and Q_T^2 by a factor $\approx$2.5–3 is an important consequence of the wave functions (55) and (56). Purely kinematically, the smaller Q^2 implies the broader range of $1/x$, and for this reason the second determination (77) may prove the more accurate one. A comparison of the two determinations (76) and (77) is an important consistency check. We conclude that from the point of view of measuring the pomeron intercept, the HERA experiments must concentrate on accurate measurements of $F_2(x,Q^2)$ and $F_L(x,Q^2)$ in the region of moderate $Q^2\lesssim 30$ GeV^2.

11. CONCLUSIONS

The purpose of this paper has been to understand the spectrum of eigenvalues of the generalized BFKL equation[4,5] for the dipole total cross section. Our emphasis was on the realistic case of finite correlation radius for the perturbative gluons and of the freezing strong coupling. The advantage of our generalized BFKL Eqs. (10) and (11) is an easy introduction of the finite gluon correlation radius in a manner which is consistent with the gauge invariance constraints.

We have shown that our generalized BFKL Eqs. (10) and (11) has a continuous spectrum which corresponds to the QCD pomeron described by the cut in the complex j-plane. We have determined the dependence on the size r of the dipole for the rightmost singularity in the j-plane and found the corresponding intercept $\Delta_{\mathbf{IP}}$. It is much smaller than that given by the BFKL formula (15) and even smaller than the lower bound cited in Ref. 9, but is substantially larger than the phenomenological value $\Delta_{\mathbf{IP}}(hN) \sim 0.1$. We have investigated the transition from GLDAP to the BFKL evolution in the limit of large $1/x$, and have shown that the two equations have an overlapping asymptotic solution in the weak-coupling limit. The phenomenologically important implication is that the GLDAP evolution with the correctly posed boundary condition remains a viable description of deep inelastic scattering well beyond the kinematical range of the HERA experiments. Nonetheless, the pomeron intercept can be determined already from the HERA data on deep inlastic scattering, and we have suggested practical methods of measuring $\Delta_{\mathbf{IP}}$.

The last two authors (B.G.Z. and V.R.Z.) are grateful to J. Speth for the hospitality at IKP, KFA Jülich.

[1] E. A. Kuraev, L. N. Lipatov, and V. S. Fadin, Sov. Phys. JETP **44**, 443 (1976); **45**, 199 (1977).
[2] Ya. Ya. Balitskii and L. N. Lipatov, Sov. J. Nucl. Phys. **28**, 822 (1978).
[3] L. N. Lipatov, Sov. Phys. JETP **63**, 904 (1986); L. N. Lipatov, in *Perturbative Quantum Chromodynamics*, ed. by A. H. Mueller, World Scientific, (1989).
[4] N. N. Nikolaev and B. G. Zakharov, Preprint 16/93, Landau Inst. (1993), Preprint KFA-IKP(Th)-1993-17, Jülich (1993), JETP **105**(5) (1994).
[5] N. N. Nikolaev, B. G. Zakharov, and V. R. Zoller, Preprint KFA-IKP(TH)-1993-34, Jülich (1993); Pis'ma v JETP **59**, 8 (1994).
[6] N. N. Nikolaev and B. G. Zakharov, Z. Phys. C **49**, 607 (1991); **53**, 331 (1992).
[7] V. Barone, M. Genovese, N. N. Nikolaev *et al.*, Preprint DFTT 28/93, Torino (1993).
[8] L. V. Gribov, E. M. Levin, and M. G. Ryskin, Phys. Rep. **100**, 1 (1983).
[9] J. C. Collins and J. Kwiecinski, Nucl. Phys. B **316**, 307 (1989).
[10] J. C. Collins and P. V. Landshoff, Phys. Lett. B **276**, 196 (1992).
[11] R. E. Hancock and D. A. Ross, Nucl. Phys. B **383**, 575 (1992).
[12] V. N. Gribov and L. N. Lipatov, Sov. J. Nucl. Phys. **15**, 438 (1972); L. N. Lipatov, Sov. J. Nucl. Phys. **20**, 181 (1974). Yu. L. Dokshitser, Sov. Phys. JETP **46**, 641 (1977). G. Altarelli and G. Parisi, Nucl. Phys. B **126**, 298 (1977).
[13] E. Shuryak, Rev. Mod. Phys. **65**, 1 (1993).
[14] G. J. Daniel and D. A. Ross, Phys. Lett. B **22**, 166 (1989).
[15] P. E. Volkovitski, A. M. Lapidus, V. I. Lisin, and K. A. Ter-Martirosyan, Sov. J. Nucl. Phys. **24**, 648 (1976); A. Donnachie and P. V. L. Landshoff, Phys. Lett. B **296**, 227 (1992).
[16] B. Z. Kopeliovich, N. N. Nikolaev, and I. K. Potashnikova, Phys. Rev. D **39**, 769 (1989).
[17] G. Marchesini and B. R. Webber, Nucl. Phys. B **349**, 617 (1991).
[18] B. Badelek, K. Charchula, M. Krawczyk, and J. Kwiecinski, Rev. Mod. Phys. **64**, 927 (1992).

This article was published in English in the original Russian journal. It is reproduced here with stylistic changes by the Translation Editor.